7-2016

Santonian—Campanian Calcareous Nannofossil Paleobiogeography

Brandi R. Moore
University of Nebraska - Lincoln, brmoore@huskers.unl.edu

SANTONIAN—CAMPANIAN CALCAREOUS NANNOFOSSIL PALEOBIOGEOGRAPHY

by

Brandi Renee Moore

A THESIS

Presented to the Faculty of

The Graduate College at the University of Nebraska

In Partial Fulfillment of Requirements

For the Degree of Master of Science

Major: Earth and Atmospheric Sciences

Under the Supervision of Professor David K. Watkins

Lincoln, Nebraska

July, 2016

SANTONIAN - CAMPANIAN CALCAREOUS NANNOFOSSIL PALEOBIOGEOGRAPHY

Brandi Renee Moore, M.S.

University of Nebraska, 2016

Advisor: David K. Watkins

Calcareous nannofossil abundance data from 11 DSDP/ODP sites were analyzed by multivariate methods to assess the paleoceanographic change that is associated with the Santonian-Campanian boundary transition. Data were divided into Santonian or Campanian age groups based on the presence or absence of the lower Campanian nannofossil species, *Aspidolithus parcus parcus*. All assemblages are dominated by *Watznaueria barnesiae, Micula decussata, and Prediscosphaera intercisa.* Analyses determined that the relative abundance of *M. decussata* generally reflects a change in temperature, with a preference for cool water. *Prediscosphaera intercisa* appears to have had an inverse abundance relationship with *M. decussata,* suggesting that *P. intercisa* exploited niche space *M. decussata* could not fill due to environmental restrictions. *W. barnesiae* exhibits no clear distribution patterns associated with temperature.

The composition of nannofossil assemblages indicates that temperature was a factor accounting for only 21.2% of the variance within the Santonian, but was

responsible for dominating 56.3% of the variance within the Campanian. The factor responsible for the most variance (35.9%) within Santonian assemblages is unknown, as it also was not dictated by nutrient availability or preservation. This study provides clarity on the paleobiogeographic environmental controls affecting nannofossil communities by demonstrating that distribution of taxa became more temperature-dependent across the Santonian-Campanian boundary.

Acknowledgments

This study used samples and data provided by the Deep Sea Drilling Program (DSDP) and the Ocean Drilling Program (ODP). The DSDP and ODP are sponsored by the National Science Foundation (NSF) and participating countries under the management of Joint Oceanographic Institutions (JOI) Inc. Support for this project was provided by the University of Nebraska-Lincoln Department of Earth and Atmospheric Sciences. I give thanks to my advisor David Watkins and committee members Sherilyn Fritz and David Harwood for providing suggestions and improving the manuscript. I also give thanks to D. Marie Weide, Bradi Gaer, Shamar Chin, and Nathan Parks, as their support and contributions to this project are greatly appreciated.

TABLE OF CONTENTS

LIST OF FIGURES AND TABLES

INTRODUCTION

Calcareous nannofossils are prolific in Cretaceous oceanic sediments. They are sensitive surface water indicators and as such can be used to reconstruct surface water conditions based on assemblage changes within samples and between geographic localities. The relative abundances of nannofossil taxa observed in sediment are commonly used to determine surface water temperature. The objective of this research is to compare Santonian calcareous nannofossil assemblages to Campanian assemblages, with emphasis on the time interval associated with the Santonian-Campanian boundary (around 83.5 million years ago), to investigate the timing and nature of the initiation of provincialism of the world oceans, as reflected in distinct high- and low-latitude nannofossil assemblages. This provinciality was more strongly expressed in the late Campanian and Maastrichtian.

The initialization of this Late Cretaceous provincialism had a profound effect on nannofossil evolution and is recorded in the biostratigraphy of oceanic sediments. It is well known that the CC biozonation scheme (Sissingh, 1977, redefined by Perch-Nielsen, 1985) for calcareous nannofossils works well for global biostratigraphic studies of sediment from the Cenomanian to the Santonian. The world's oceans throughout most of the Cretaceous were relatively uniform, allowing a single zonation scheme to be viable for both high- and low-latitude nannofossil assemblages. Yet numerous studies on Upper Cretaceous nannofossils have documented the absence of marker species at high latitudinal sites, which renders the CC zonation scheme useless for Campanian and

Maastrichtian high-latitude assemblages (Thierstein, 1981a; Watkins et al., 1996; Lees 2002).

By the end of the Campanian, there was a strong provinciality within ocean nannoplankton communities that reflected a strong paleolatitudinal temperature gradient (Thierstein, 1981a). Some nannofossil species exhibited distinct shifts from wide latitudinal ranges in the late Santonian to shorter ranges restricted to low latitudes within the Campanian. For example, *Watznaueria barnesiae* had high abundances in both high and low latitudes throughout most of the Cretaceous, but by the end of the Campanian, it became restricted to low latitudes, and its percent abundance decreased significantly in sediments deposited closer to the poles. While some species became restricted to low latitudes, net speciation events of high latitude taxa also occurred, leading to a distinctive subpolar nannofossil association (Huber and Watkins, 1992). By the Maastrichtian, a strong paleolatitudinal gradient was evident in the relative abundances of nannofossil species within assemblages.

In order to investigate the initiation of the Campanian paleobiogeographic division of the world's oceans, nannofossil assemblage changes across the Santonian-Campanian boundary were examined from multiple sites around the world. Potential differences in composition and structure of nannofossil paleocommunities were observed by recording assemblage data, including individual nannofossil taxon absolute and percent abundances within assemblages. Statistical and numerical analyses (including Shannon-diversity and eigenvector extraction methods) were applied to the data to evaluate variations in abundance patterns and document presences and absences of tropical and

high latitude taxa. This study serves to document if and how Santonian nannofossil assemblages differ from Campanian assemblages and to determine the environmental factors responsible for any variations, with emphasis on surface water temperature.

LOCALITIES

Samples from 11 localities (Figure 1) were examined from Deep Sea Drilling Project (DSDP) and Ocean Drilling Program (ODP) sites. Sites were chosen based on their stratigraphic completeness, their collective range in latitude, and by the suggestion of relevant ages (late Santonian and/or early Campanian) in initial DSDP/ODP reports. Lithologic and stratigraphic descriptions of these sites have been previously published and are summarized in Table 1.

A paleogeographic reconstruction (Figure 2) was produced for the Santonian-Campanian boundary (83.5Ma), depicting past positions for all localities (Hay et al., 1999). The reconstruction places all sites except Leg 10 Site 95 at more southerly latitudes than their present-day locations. Paleolatitudes of all sites were used to determine high- or low- latitudinal positions as applied in the paleobiogeographical analysis and discussion later in this study.

MATERIALS/METHODS

Smear slides for samples from sites 167, 305, 310, 357, 363, 369, 462, and 762 were prepared using the double slurry method of Watkins and Bergen (2003), shown to generate reproducible abundance data at the 99.99% confidence level. Samples from

sites 95, 738, and 750 were previously prepared. All slides were viewed on an Olympus BX51 light microscope at 1000-1250x magnification using plane polarization (PPL), cross polarization (XPL) and a one-quarter λ gypsum plate.

Nannofossil biostratigraphic and assemblage data were collected by counting >456 specimens to produce accurate abundance data at the 95% confidence level (Chang, 1967). Whole and half coccolith specimens were counted. Specimens <2µm were not counted, as their classification at the species level was not readily possible. The slides were also scanned for 200-400 more fields of view to identify rare marker species for biochronologic constraints. Nannofossil preservation was determined based on criteria described in Watkins (1992). Numerical and statistical analyses of collected nannofossil abundance data were conducted using PAST (Paleontology Statistics) software (Hammer et al., 2001).

RESULTS

A total of 121 nannofossil taxa were identified from all sites combined. Most samples yield moderately well preserved to poorly preserved nannofossils. Only 5 samples from those observed (4 from Leg 39-357, 1 from Leg 41-369) have moderate-good preservation. As a result of poor preservation, only 74 of the 151 samples were counted for numerical and statistical analysis (Table 2). Individual sample richness ranges from 20-48 species. The Shannon diversity of all counted samples (H) ranges from 1.56-3.03, with an average of 2.36.

Leg 40 Site 363 was not included in analyses, graphs or correlations. This site only has 1 countable sample from 7 selected across the Santonian-Campanian boundary. Abundance data from the sample are dominated by over 66% *Micula decussata*, which affected the robustness of the PAST analyses. Specimens are severely overgrown, indicative of diagenetic alteration. The high percentage of *M. decussata* could be a result of multiple factors. One possibility is of a cold eastern ocean boundary current, where cold water circulates in a counter clockwise direction in the Southern Hemisphere, bringing cold water from more southerly high latitudes into lower latitudes along the western edge of Africa. Site 363 is located in the South Atlantic Ocean on the south east corner of the Angola Basin, within close proximity of the western edge of the African continent. This cold ocean current is also linked to the possibility of upwelling occurring along the western continental boundary. The boundary current pulls water away from the continental edge, allowing deep bottom water to rise to the surface, bringing cooler, turbulent water, and nutrients with it. *M. decussata* may have thrived in cold surface waters that were brought to this latitude as a result of ocean currents or a coastal upwelling zone. A third possibility for the high relative abundance of *M. decussata* is diagenesis. *M. decussata* is dissolution resistant, and the robust morphology usually exhibits overgrowth while other species dissolve. Thierstein (1981a) also notes that where *W. barnesiae* decreases in low latitudes, *M. decussata* increases, and attributes the switch to differential sensitivity to poor preservation conditions. It should be acknowledged that an explanation of such a high percent abundance of this species could come from a combination of any of the aforementioned factors.

BIOSTRATIGRAPHY

Calcareous nannofossil biozonal marker species were used to distinguish between Santonian and Campanian samples. The Cretaceous Coccoliths (CC) zonation scheme from Sissingh (1977) places the calcareous nannofossil Zone CC17 at the Santonian-Campanian boundary, defined by the First Appearance Datum (FAD) of *Calculites obscurus* (Deflandre 1959) Prins and Sissingh *in* Sissingh 1977. In this scheme, the base of CC18 is defined as the FAD of the *Aspidolithus parcus* (Stradner 1963) Noel 1969 group and is placed within the lower Campanian. Sissingh's zonal scheme was later modified by Perch-Nielsen (1985), who keeps *Aspidolithus parcus parcus* as the marker species for CC18, but places the base of the zone at the Santonian-Campanian boundary, pushing the base of CC17 into the upper Santonian (this scheme also keeps *C. obscurus* as the CC17 marker). Burnett (1998) uses a different nannofossil zonation scheme for this interval, the Upper Cretaceous (UC) nannofossil zonation, which uses *A. parcus parcus* as the marker species for Zone UC14. This zone is placed within the lower Campanian, similar to Sissingh's initial CC zones, instead of at the boundary as in Perch-Nielsen's modification. Burnett's scheme also introduces *Arkhangelskiella cymbiformis* Vekshina 1959 as the marker for Zone UC13 within the lower-Campanian, just above the Santonian-Campanian boundary.

The nannofossil biozonation scheme used in this study is from the age model provided by Time Scale Creator (Ogg et al., 2012). This age model combines aspects of the CC and UC zonal schemes described above. The FAD of *A. parcus parcus* is still used as the marker species for Zone CC18, but it is placed within the lower Campanian. Zone

CC17 is still marked by the FAD of *C. obscurus*, but the base of this zone is placed within the uppermost Santonian. *A. cymbiformis* is not used as a specific zonal marker, but the FAD is included in the lowermost Campanian. Blair and Watkins (2009) and Kita (2015) demonstrate that the FAD of *A*. *cymbiformis* occurs well below the boundary; therefore, it is not used as an indicator for the Campanian in this study. *C. obscurus*, was not useful for determining upper-Santonian samples, as it was only observed in 8 of the counted samples, and all counts totaled less than 10 specimens per sample.

Any sample containing *A. parcus parcus*, or any younger marker species after CC18, is assigned to the Campanian. Based on these criteria, 23 samples are identified as Santonian, and 51 are identified as Campanian (Table 3). The mid-late Campanian has been recognized in this study as CC21 or younger (Sissingh, 1977; Perch-Nielsen, 1985), with the occurrences of abundant *Ceratolithoides* Bramlette & Martini 1964 species and *Uniplanarius* Hattner & Wise 1980 species. Not all samples were placed readily into the CC zonation scheme, as the absence of marker species made it difficult. This is explained in more detail in the discussion.

PALEOBIOGEOGRAPHY

A temperature index was created based on nannofossil species with known temperature preferences to determine if changes in surface water paleotemperature occurred during the late Santonian or early Campanian. Percent abundances of 7 species were used to determine the Temperature Index (TI). The following species were chosen based on their age ranges, which persist through the late Santonian and Campanian:

Watznaueria barnesiae, Ceratolithoides serratus, Ahmuellerella octoradiata, Arkhangelskiella cymbiformis, Eiffellithus turriseiffelii, Micula decussata, and *Reinhardtites anthophorus* (see Discussion for explanation of taxon temperature preferences).

Sites were categorized into climate zones based on paleolatitude. Since the modern oceanic provinciality is not analogous to the warmer Cretaceous climate, modern climate zones were not used. During the Late Cretaceous, a paleotemperature gradient existed from the poles to the equator, with a suggested magnitude somewhere between 32^{o}C – 12^{o}C; whereas the modern temperature gradient is ~35^{o}C (summarized in Barron, 1983; Barron et al., 1993; Pearson et al., 2001; Lees, 2002; Hay, 2008). The weaker paleotemperature gradient between the poles and the equator in the Cretaceous results in broader ranges of relatively uniform warm-water nannofossil assemblages, with distinct high-latitude assemblages appearing abruptly across water mass boundaries. Street and Bown (2000) observed high-latitude nannofossil assemblages >50^{o} N and S from the Berriasian to the Barremian. Roth and Bowdler (1981) observed high latitude mid-Cretaceous assemblages that are restricted to >40^{o} N and S. Upper Campanian – Maastrichtian assemblages are strongly provincial, reflecting gradual changes in warm and cool-water taxa spanning all latitudes (Thierstein, 1981a; Huber and Watkins, 1992). The weak temperature gradient in the Lower and middle Cretaceous, and the stronger gradient in the Upper Cretaceous make it possible to split the high and low paleolatitudinal regions at 30^{o} latitude in this study. Sites 95, 369, 305, 310, 167, and 462 are considered “low-latitude” sites, and Sites 363, 357, 762, 750, and

738 are considered “high-latitude” sites based on their paleolatitudes relative to 30^{o} (Figure 2).

Watznaueria barnesiae is the most abundant species in virtually all samples. Percent abundances range from 17.4%-51.9%, with an average abundance of 32%. There is no clear correlation of *W. barnesiae* abundance to paleolatitude in the current study. *Prediscosphaera intercisa* generally comprises >20% of low-latitude assemblages, and 10-20% of high-latitude assemblages. *Micula decussata* abundance varies: it comprises less than 1% of some assemblages and up to 33% of others, but generally comprises less than 10% of the assemblages in low latitudes and greater than 15% in high latitudes. *Cribrosphaerella ehrenbergii* comprises up to 10% of some assemblages, averaging 5% for all samples. No other species makes up more than 6% of assemblages.

Calcareous nannofossil abundance data were analyzed using CABFAC factor analysis and Principal Component Analysis (PCA) in PAST to find factors responsible for variance within the data. CABFAC analysis on all data indicates that a majority (85%) of the variance is explained by one factor (Factor 1). The only significant species associated with Factor 1 is *Prediscosphaera intercisa* with a loading value of 9.48. The second highest factor explains 6.8% of the variance and is too low for any practical explanations. CABFAC factor analyses result in a maximized shared portion of variance; therefore, Principle Component Analyses were also used on the data. PCA results maximize the total variance of observed variables.

The PCA results of all data indicate that 44.5% of the variance can be explained by one principal component (PC1). The two significant loadings linked to PC1 are *Micula decussata* (0.57) and *Prediscosphaera intercisa* (-0.75).

PC2 through PC4 are not responsible for much variance (16.6% and less) and are not considered practical to explain; therefore, interpretations are not pursued for these components. Data were then divided into the two stages, and CABFAC factor analyses and principal component analyses were run separately on Campanian and Santonian data.

The CABFAC factor analysis on Campanian data produced one significant factor responsible for 88.5% of the variance. The only significant species associated with Factor 1 in the Campanian is *P. intercisa,* with a loading value of 9.3.

The Principal Component Analysis of Campanian data produced three statistically significant components. PC1 is responsible for 56.3% of the variance within the data. Significant loadings differ from the CABFAC results in that they include *M. decussata* (0.69) along with *P. intercisa* (-0.67). PC2 (20.6%) and PC3 (8.9%) do not explain as much variance as PC1; therefore, interpretations are not pursued for these components.

The CABFAC factor analysis on Santonian data resulted in one significant factor responsible for 84% of the variance present. Three species are associated with Factor 1 with significant loadings: *M. decussata* (-4.0), *P. intercisa* (5.9), and *W. barnesiae* (5.2).

The Principal Component Analysis of Santonian data produced four statistically significant components. PC1 accounts for 35.9% of the variance. The significant loadings include *H. trabeculatus* (0.70) and *P. intercisa* (-0.47). PC2 is responsible for 21.2% of the

variance within the data. The single significant loading is *M. decussata* (-0.64). The variance reflected by PC3 (14.6%) and PC4 (12%) are not considered practical to interpret.

DISCUSSION

BIOSTRATIGRAPHY

Assignment of samples to nannofossil CC biostratigraphic zones was not possible for most samples because of the absence of marker species through the interval. The CC17 marker species *Calculites obscurus* is extremely rare in the dataset. It was observed in only 8 samples, and total counts per sample were never greater than 10 specimens. *Arkhangelskiella cymbiformis* was present in 18 samples but was not used to distinguish lower Campanian assemblages in this study. Blair and Watkins (2009) and Kita (2015) discovered that the first occurrence of this species is well below the basal Campanian boundary, contrary to what was proposed by Burnett (1998). Since this is not a high-resolution biostratigraphic study, new marker species are not proposed for CC17. Results from this study differ slightly from previous results, as not all marker species were observed here as in the other studies. Summarized age assignments of samples in this study are in Table 3.

Countable samples from Site 95 are all assigned to the Santonian based on the lack of *Aspidolithus parcus parcus*. These results differ slightly from the DSDP report, which lists samples from cores 13 and 14 as containing *A. parcus parcus* (=*Broinsonia parca*) and were placed into the lower Campanian. Core 15 samples were placed into

the Santonian (Bukry, 1973). Ambiguity within the *Broinsonia*/*Aspidolithus* genera in the past is the likely cause of the difference in identification of this species.

All counted samples from Site 167 are placed into the mid-late Campanian (from cores 55 and 56). The DSDP report lists samples from cores 55, 56, and 57 as lower Campanian and samples from cores 58 and 59 as Coniacian- Santonian. The author's criterion for placing cores 55 and 56 into the lower Campanian was the presence of *Ceratolithoides aculeus* (Stradner 1961) Prins & Sissingh *in* Sissingh 1977, which is the basis for the middle Campanian in the current study.

Most samples from Site 305 are determined to have mid-upper Campanian assemblages (from cores 25-27) based on the presences of common *Uniplanarius* and *Ceratolithoides* species. Samples from sections 305-28-1 and 28-2 are assigned to the lower Campanian based on the presence of *A. parcus parcus,* but lack *Uniplanarius* or *Ceratolithoides* species. The DSDP report placed samples from cores 25-27 into the lower Campanian, and samples from core 28 into Coniacian-Santonian; however, they did not distinguish which taxa were used for placement into stages (Bukry, 1975).

Most samples from Site 310 are determined to be mid-upper Campanian (from cores 16-20) based on the presence of common *Uniplanarius* or *Ceratolithoides* species. Samples from sections 310-20-2,-3,-4 are placed into the lower Campanian based on the absence of *Uniplanarius* and rare *Ceratolithoides*. The DSDP report states that all samples from this interval are lower Campanian (Bukry, 1975).

All but two samples from Site 357 are assigned to the lower Campanian (in sections 357-39-1 through 357-43-1) based on the presence of *A. parcus parcus*. The

remaining two samples from sections 357-43-5 and -6 are considered Santonian, because they lack *A. parcus parcus*. The DSDP nannofossil report has slightly different results based on the occurrence of *Marthasterites furcatus* with *A. parcus parcus*. Samples from cores 39 and 40 were placed into the lower Campanian based on the presence of *A. parcus parcus (Broinsonia parca)* and the absence of *M. furcatus*. Samples from cores 40 and 41 were placed into the upper Santonian based on the co-occurrence of *A. parcus parcus* and *M. furcatus*. Samples from cores 42 and 43 were considered Coniacian-Santonian based on the lack of *A. parcus parcus*. (Perch-Nielsen, 1977).

Only one sample has been counted from Site 363 within section 363-23R-2W, and it is assigned to the mid-upper Campanian based on the presence of *Uniplanarius gothicus*. The DSDP report notes *A. parcus parcus* was used to split samples from cores 23 and 24 from 25 and placed them into the Campanian and Santonian, respectively (Proto Decima et al., 1978).

Samples from Site 369 contain mid-upper Campanian assemblages in sections 369A-39-2 and -3 based on the presence of *Uniplanarius gothicus*. Lower Campanian assemblages were observed in section 369A-40-1 containing *Aspidolithus parcus constrictus*. Santonian assemblages were observed in section 369A-40-4 based on the absence of the aforementioned taxa. The DSDP report states that samples from section 369A-39-3 were also determined to be upper Campanian but placed the sample from core-catcher of core 39 into the lower Campanian. Upper Santonian assemblages were

not observed, and sections 369A-41-2 through 40-3 were placed into the Coniacian-Santonian (Cepek, 1977).

Counted samples from core 55 from Site 462 are assigned to the lower Campanian based on the presence of *A. parcus parcus* and *A. parcus constrictus*. Samples from core 58 are placed into the Santonian, because they lack *A. parcus parcus*. The DSDP report lists the same age for samples from core 55 (as lower Campanian) based on the presence of *A. parcus parcus* but claims samples from cores 56-58 are Turonian-Santonian based on vague ranges of *M. decussata* and *Eprolithus floralis (Lithastrinus floralis* in text; Thierstein, 1981b).

The only counted sample from Site 738 is determined to be Santonian, as *A. parcus parcus* was not observed. The ODP report also lists this sample as Santonian (Wei and Thierstein, 1989). The ODP report assigned samples from core 26 into the upper Campanian-Maastrichtian based on the presence of *A. parcus parcus*; however, all samples from cores 24-29 in the current study were not countable.

All counted samples from Site 750 are placed into the Santonian, as *A. parcus parcus* was not observed (though *A. parcus expansus* was observed). Watkins (1992) assigned samples from cores 8 and 9 and sample 10W-1, 36-38cm to the Lower Campanian based on the presence of *A. parcus parcus* and samples 10W-1, 48-50cm, and 80-81cm to the Santonian.

Samples from core 61 from Site 762 are assigned to the Lower Campanian based on the presence of *A. parcus parcus*. Samples from cores 62 to 64 are determined to be Santonian, because they lack *A. parcus parcus*. Bralower and Siesser (1992) assigned

samples from sections 61X-1 through 63X-1 to the lower Campanian based on the presence of *A. parcus parcus (B. parca*) and sections 63X-1 to 66X-CC to the upper Santonian because that species was not observed. The main difference between studies is the placement of samples in sections 62X-1 to 63X-1. *A. parcus parcus* was not observed in the current study; therefore, samples from these sections were not placed into the lower Campanian.

PALEOBIOGEOGRAPHY

A paleotemperature index was created to determine the relative percent abundances of cool- or warm-water taxa within assemblages. The resulting values serve as a proxy to determine whether the assemblages observed reflect cool or warm surface-waters. By the end of the Campanian, there was a strong provinciality within ocean nannoplankton communities that reflected a strong paleotatitudinal thermal gradient (Thierstein, 1981a). The provinciality resulted in a distinctive subpolar nannofossil association. Formerly cosmopolitan species became restricted to low latitudes concomitant with the net speciation of high-latitude taxa with affinities for those cooler waters (Huber and Watkins, 1992). The temperature index (TI) was calculated by dividing the percent of warm-water taxa by the sum of the percent of warm- and cool-water taxa as follows:

$$TI = \frac{[\%\, C.serratus\ +\ \%\, W\,.barnesiae]}{[\%\, C.serratus\ +\ \%\, W.barnesiae]\ +\ [\%\, A.octoradiata\ +\ \%\, A.cymbiformis\ +\ \%\, E.turriseiffelii\ +\ \%\, M.decussata\ +\ \%\, R.anthophorus]} * 100$$

Watznaueria barnesiae (Black *in* Black and Barnes 1959) Perch-Nielsen 1968 was ubiquitous throughout the Cretaceous, but became increasingly less abundant in high latitudes by the Maastrichtian (Watkins et al., 1996, Thierstein, 1981a). Its abundance became restricted to lower latitudes, with abundances greater than 30% in low latitudes and less than 2% at high latitudes, expressing an affinity for warm water (Thierstein, 1981a).

Cylindralithus serratus (Bramlette and Martini 1964) Stover 1966 has been observed to be the most ubiquitous in low-latitude assemblages, implying an affinity for warm water (Thierstein, 1981a). Thierstein states that this species makes up 2-10% of the assemblages and had an affinity for open ocean waters.

Ahmuellerella octoradiata (Górka 1957) Reinhardt & Górka 1967 is indicated by many to have had an affinity for cool water (Thierstein, 1981a; Watkins, 1992; Watkins et al., 1996; Pospichal and Wise, 1990; Lees, 2002).

Arkhangelskiella cymbiformis Vekshina 1959 also was observed by many to have had an affinity for cool water (Thierstein, 1981a; Watkins, 1992, Lees 2002). Thierstein (1981a) documents this species as 10-20% of the assemblage in high latitudes.

Eiffellithus turriseiffelii (Deflandre in Deflandre & Fert 1954) Reinhardt 1965 is a cool water indicator and averages ~10% of abundances in high-latitude assemblages (Thierstein, 1981a; Watkins, 1992).

Reinhardtites anthophorus (Deflandre 1959) Perch-Nielsen 1968 is considered as having a cool water affinity, comprising 10% of austral assemblages (Thierstein, 1981a, Linnert et al., 2011).

Micula decussata (Gardet 1955) Vekshina 1959 is observed as a cool-water indicator (Watkins, 1992; Watkins and Self-Trail, 2005). Thierstein (1981a) documented assemblages consisting of >40% of this species in the subtropics but does suggest it is an indicator of preservation over temperature.

ANALYSIS

The CABFAC factor analysis result of calcareous nannofossil abundance data (Factor 1) has a strong positive correlation (Figure 3) with the Temperature index (TI); therefore, the variable explained by Factor 1 is most-likely controlled by surface water temperature. As temperature increases, Factor 1 increases ($r = 0.71$, $p = 2.6 \times 10^{-12}$). The highest loading on Factor 1 (*P. intercisa*, 9.38) has a correlation coefficient to Factor 1 of 0.92 ($p = 3.27 \times 10^{-30}$). *P. intercisa* has a lower correlation coefficient with TI ($r = 0.56$), but the probability that they are uncorrelated is very low ($p = 4.5 \times 10^{-2}$).

The result of the principal component analysis of abundance data (PC1) is strongly correlated to the temperature index ($r = 0.78$), suggesting that the variable responsible for PC1 is also indicative of surface water temperature (Figure 4). The same temperature index used in the CABFAC analysis was used here. The significant loadings for PC1, *Micula decussata* (0.57) and *Prediscosphaera intercisa* (-0.75), indicate that as PC1 increases, the abundance of *M. decussata* increases ($r = 0.80$, $p = 4.26 \times 10^{-17}$) and *P. intercisa* decreases ($r = -0.92$, $p = 4.94 \times 10^{-31}$). *M. decussata* is a well-known temperature indicator of cool water, which was the basis for choosing to include it in the temperature index calculation. *P. intercisa* is a ubiquitous species with no well-

documented preference for certain temperatures. Since these species inversely co-vary as PC1 changes, and if PC1 is assumed to be temperature, *P. intercisa* can initially be inferred as a warm-water taxon. However, combining the Santonian and Campanian data obscures the potential presence of a change in community structure across the boundary. Therefore, individual stage-level CABFAC factor analyses, Principal Component Analyses, and correlation results should be taken into account.

Factor 1 of the CABFAC factor analysis for Campanian data is strongly correlated to the TI ($r = 0.83$). As in the combined data results, the only significant species associated with Factor 1 in the Campanian is *P. intercisa* (9.3). *P. intercisa* abundance is strongly correlated with Factor 1 ($r = 0.88$, $p = 2.0x10^{-17}$). Though not a loading on Factor 1, comparison of the distribution of known cool-water indicator *Micula decussata* to Campanian Factor 1 yields a negative high confidence correlation ($r = -0.92$, $p = 4.57x10^{-21}$). This strong correlation, along with the inverse relationship of this taxon to *P. intercisa*, corroborates that Campanian Factor 1 is most likely related to paleotemperature.

The Principal Component Analysis results (PC1) of the Campanian data are more strongly correlated to TI values among Campanian samples ($r = -0.86$, $p = 1.5x10^{-15}$, Figure 5) than among all data combined. Similar to the combined stage PCA, Figure 5 illustrates that the abundances of the two species with the highest loadings in PC1 (*M. decussata:* 0.68 and *P. intercisa:* -.067) also are highly correlated with PC1. ($r = 0.93$, $p = 6.09x10^{-22}$; $r = 0.91$, $p = 3.02x10^{-20}$, respectively). As described above, this inverse relationship implies *P. intercisa* has a warm-water preference. *M. decussata* abundances

are highest in samples from high-latitude sites, and *P. intercisa* appears to increase in abundance from high- to low-latitude sites.

The results of the CABFAC factor analysis for Santonian data (Factor 1) appear to be temperature-driven, with a correlation coefficient of 0.71 ($p = 1.4x10^{-04}$). Comparison of the species' abundances with the highest loadings on Factor 1 to Factor 1 indicates they are not well correlated. *M. decussata* is only marginally correlated with Factor 1 ($r = -0.60$, $p = 2.6x10^{-}3$).), but *P. intercisa* yields a low confidence correlation to Factor 1 ($r = 0.46$, $p = 0.03$). *W. barnesiae* abundance values are not correlated to Factor 1 at all ($r = 6.2x10^{-04}$, $p = 0.99$). Based on the low confidence correlations of the loadings on Factor 1, it is suggested that the CABFAC analysis is obscuring results by combining variables that may be responsible for different magnitudes of variation within the dataset.

The Principle Components Analysis values for Santonian samples (PC1) do not correlate well with TI values ($r = 0.30$, $p = 0.17$; Figure 6). In general, low-latitude Santonian assemblages have higher TI values than high-latitude assemblages, but PC1 values show similar ranges between latitudes. The species' abundances with significant loadings on PC1 have a high correlation to PC1 values (*H. trabeculatus:* $r = 0.85$, $p = 2.05x10^{-07}$; *P. intercisa:* $r = -0.72$, $p = 1.14x10^{-04}$). To our knowledge, no studies have been done on the paleoecological preferences of *H. trabeculatus.* Watkins (1992) observed a short-lived, abrupt increase in the abundance of this species just before the basal Campanian boundary in high southern latitudes. This abrupt increase in abundance yielded counts greater than 100 specimens per sample, but this species is only found in 2 samples in the current study (within sections 738C-27R-5 and 750B-

10W-1). Therefore, it is still unclear what may be responsible for the short term 'bloom' of *H. trabeculatus* and how it relates to the controlling environmental factors at this time.

Nutrient availability has been considered as a governing environmental factor in Santonian assemblages, but it does not explain the variance of PC1. Only one Santonian sample has evidence of increased fertility of surface-waters. The increased relative abundances of *Biscutum* spp. and *Zeugrhabdotus* spp. (*Zygodiscus* in past studies) in Lower and middle Cretaceous assemblages are suggested by many to indicate nutrient-rich surface waters (Roth and Bowdler, 1981; Roth and Krumbach, 1986; Watkins, 1989; Erba, 1992; Williams and Bralower, 1995; Street and Bown, 2000). Generally when present, these taxa tend to show an inverse relationship with *W. barnesiae* abundance. However, *Biscutum* spp. and *Zeugrhabdotus* spp. are uncommon in assemblages observed in this study. Only one sample has a total *Biscutum* abundance of 6% (357-39R-1W, 36-37cm), but this sample has been placed into the lower Campanian. Two Santonian samples have *Biscutum* abundances of 3% (369A-40-4, 84-85cm, and 462-58-4, 74-75cm). Four samples have abundances of 2%, and all other abundances of *Biscutum* spp. were <1% where present. *Zeugrhabdotus* spp. are also uncommon in observed assemblages. *Zeughrabdotus* spp. comprises 5% of the assemblage from Santonian Sample 369A-40-4, 84-85cm and comprises 2% of the assemblage in two other samples. The rest of the assemblages have abundances <1% where present. Only one sample appears to have a Santonian assemblage that reflects an increase of surface-water fertility in comparison with the rest of the assemblages. The 5%

Zeugrhabdotus abundance and 3% *Biscutum* abundance in sample 369A-40-4, 84-85cm is mirrored by a low abundance of 18% *W. barnesiae* (compared to the average of 32% in all assemblages) and the relatively low abundances of *M. decussata* (0%) and *P. intercisa* (13%). Similarly, the 6% *Biscutum* abundance in Campanian sample 357-39R-1W, 36-37cm is reflected by a relatively low *W. barnesiae* abundance of 18%, and interestingly, a low *M. decussata* abundance of 7%, but average *P. intercisa* abundance of 22%. Site 369 is located on the continental slope of Cape Bojador close to the coast of the Western Sahara. The presence of high-fertility indicator species suggests that the close proximity of the shore to the site influenced nutrient levels in the surface-waters, at least for part of the Santonian. Yet overall, almost 36% of the variance observed within Santonian assemblages (PC1) does not stem from the abundance of nutrient-indicative genera. Apart from their increased abundance in sample 369A-40-4, 36-37cm, they make up less than 1% of the majority of assemblages, and thus cannot affect variation significantly.

Diversity of assemblages was also examined to evaluate the cause of variance among nannofossil assemblages in the Santonian. Low diversities could be related to poor preservation of coccoliths within sediment, where most species' coccoliths dissolve or become unidentifiable. Diversity differences among Santonian assemblages are not responsible for the variation observed in PC1 (Figure 6), as diversity values are uncorrelated with PC1 values ($r = 0.02$, $p = 0.94$). The two outliers in the high-latitude data are two samples that are comprised of abnormally high *Helicolithus trabeculatus* abundances (38% in Sample 738C-27R-5, 67-68cm and 21% in Sample 750B-10W-1, 48-

50cm). These two samples also have very low *M. decussata* abundances (2% and 7%, respectively), despite being from the highest-latitude sites (>60^{o}). It is possible that *H. trabeculatus* reflects surface-water fertility, since abundances relative to *M. decussata* behave similarly to *Biscutum* and *Zeugrhabdotus*; however, high *H. trabeculatus* abundance does not mirror low *W. barnesiae* (29% and 32% in the samples, respectively) as is usually the case in high fertility surface-water assemblages. Diversity is also considered to be reflected by *W*. *barnesiae* abundance. *W. barnesiae* is most commonly the most dissolution-resistant taxa within nannofossil assemblages (Thierstein, 1981a; Roth and Bowdler, 1981; Roth and Krumbach, 1986); however, diversity values for all samples only correlate marginally with *W. barnesiae* abundances ($r = -0.48$, $p = 0.02$). This confirms that the variance reflected in PC1 is probably not related to the diversity of assemblages or to preservation. Temperature, nutrients, and diversity are not related to the 35.9% variance reflected in PC1 during the Santonian; therefore, no explanation can be given for the factor responsible for this variance at this time.

The second principal component (PC2) within the Santonian data is interpreted as showing variance within the data related to paleotemperature, as PC2 strongly correlates with TI ($r = 0.89$, $p = 1.13 \times 10^{-08}$, Figure 7). The single significant loading on PC2 is the cool-water taxon, *M. decussata*, and its abundance correlates strongly to TI ($r = -0.84$, $p = 7.18 \times 10^{-07}$). CABFAC Factor 1 results of Santonian assemblages also correlate strongly with the Santonian PC2 values ($r = 0.90$), and not very much to PC1 ($r = -0.24$). However, PC2 is only responsible for 21.2 % of the variance within the data, so while

temperature appears to have a small effect on Santonian assemblages, the nannofossil paleocommunity compositions are dominated by some other factor.

Not all of the temperature indicator species chosen for the temperature index calculation clearly exhibit expected trends. In Campanian assemblages, only *Reinhardtites anthophorus* and *Micula decussata* have high abundances at the highest latitudes, indicative of cool surface water (Figure 8). The rest of the cool-water taxa, and the warm-water indicator *Watznaueria barnesiae* show no preference, as their respective abundances remain relatively uniform through all latitudes. *Prediscosphaera intercisa* exhibits slightly higher abundances in low-latitude sites. The warm-water species *Cylindralithus serratus* is generally more abundant in low-latitude sites.

In Santonian assemblages, all cool-water indicators follow expected trends with higher abundances in higher latitudes, except *Eiffellithus turriseiffelii (Figure 9)*. *E. turriseiffelii* exhibits a peak in abundance in the lowest latitudes. *P. intercisa* has slightly higher abundances in higher latitudes, opposite of its trend observed in the Campanian. *C. serratus* and *M. decussata* abundances are relatively uniform across a broad latitudinal range. Broader ranges of these taxa, especially *M. decussata*, may indicate a weak paleolatitudinal temperature gradient, relative to their Campanian distributions, which exhibit a pronounced cool-water affinity at the highest latitudes.

The dominance of *W. barnesiae* in all assemblages does not appear to reflect changes in temperature. Street and Bown (2000) suggest *W. barnesiae* is r-selected based on its ubiquitous occurrence through different ecological environments. Though *W. barnesiae* is dominant in the current study by an equal percentage in both high and

low-latitude assemblages (averaging 31% and 32% in high and low Campanian samples, respectively, and 34% to 32% in high and low Santonian samples, respectively), it is accompanied by high percentages (24%) of *P. intercisa* in Campanian low-latitude assemblages. *P. intercisa* only comprises an average of 13% of Campanian assemblages at high latitudes. Santonian percentages of *P. intercisa* abundances have a less stark difference: averaging 9.5% in low latitudes to 13.6% in high latitudes. If assemblages are temperature-driven in the Campanian, the stable percentage of *P. intercisa* at high latitudes across the boundary and the increase in *P. intercisa* abundance in low-latitude samples across the boundary may reflect an external factor responsible for *P. intercisa* distribution not related to temperature within the Santonian.

There has been little work done on the genus *Prediscosphaera* Vekshina 1959, and this is particularly problematic when identifying species for biostratigraphic correlation. Throughout the Upper Cretaceous, this genus comprises upwards of 15% of assemblages (this study; Watkins and Self-Trail, 2005; Blair and Watkins, 2009). The most commonly used species in literature is *P. cretacea* (Arkhangelsky 1912) Gartner 1968, which is described as an oval coccolith with two rims of slightly different widths comprised of 16 petaloid elements. The central area is spanned by 4 bars that do not run parallel to the major and minor axes of the coccolith but create an X. *Prediscosphaera intercisa* is described similarly to *P. cretacea*, but they are differentiated in this study based on the characteristics of the diagonal crossbars (Figure 10, images 9 and 10). *P. intercisa* has solid bars connecting to the inner cycle. *P. cretacea* has two layers of crossbars, which appear as a split single bar in polarized light (as

described by Gartner, 1968). Perch-Nielsen (1985) also suggests that *P. cretacea* evolved from *P. intercisa* within the Campanian (within CC18). Based on this differentiation, very few *P. cretacea* specimens were identified in this study, and it comprises <1% of assemblages where present. With poor preservation, the difficulty discerning *P. cretacea* from *P. intercisa* may have resulted in skewed counts towards *P. intercisa*. Regardless, results of this study show that *P. intercisa* makes up an average of 19% of assemblages (ranging from <1% to 39%), which is comparable to *P. cretacea* abundances in other studies. It is inferred that the *P.intercisa* of this study is what others refer to as *P. cretacea*.

Prediscosphaera intercisa was not used as a temperature indicator, because there has not been uniform identification of this species in the past; however, other studies suggest *P. cretacea* exhibits distribution patterns related to temperature. Wind (1979) states that paleogeographic distributions of this species indicate it has a cool-water preference. Watkins (1992), Wise (1983), and Pospichal and Wise (1990) indicate that there are higher abundances of this species at higher latitudes. Thierstein (1981a) illustrates that the distribution of *P. cretacea* has no clear pattern related to changes in temperature. Mitchell (2012) describes morphotypes of early *Prediscosphaera* forms that radiated in response to warm temperatures. Mitchell also suggested that the morphotypes exploited decreased stratification of the water column and increased fertility of surface waters; therefore, *P. intercisa* could be inferred to overtake niche space as it becomes available. The exploitation of niche space could be responsible for the inverse relationship observed in the current study between *P. intercisa* and *M.*

decussata in the Campanian, and could explain why Santonian samples have relatively the same abundances of both species at high latitudes, but more *P. intercisa* (9.5%) than *M. decussata* (1.2%) in low latitudes.

The poor preservation of virtually all samples suggests something significant was occurring in marine settings during the early Campanian. A study by Jarvis et al. (2006) includes a $\delta^{13}C$ curve through the Santonian-Campanian boundary. They identified a "Santonian-Campanian boundary event," which reflects a positive isotope excursion (values up to +2.9‰) across the boundary. The increase of $\delta^{13}C$ is correlated to transgressions of marine environments during the early Campanian. Reworking of sediments from increasing sea levels results in possible erosion or dissolution of deposited sediments, ultimately resulting in disconformities within the sediment record. Reworking can also result in increased productivity in the surface waters, enhanced carbon burial rates, and tend to result in lower nannoplankton abundances. Although these results were observed in locations around Europe, if these processes were occurring globally, it could account for low diversity, poor preservation, or disconformities present within upper Santonian and lower Campanian sediments observed in this study.

CONCLUSIONS

High-latitude calcareous nannofossil assemblages are present in Santonian and lower Campanian sediments. All assemblages are dominated by *Watznaueria barnesiae,* shown here to be ubiquitous in both high and low-latitude assemblages. Results from

principal component analyses indicate that *Micula decussata* follows an expected trend as a cool-water temperature indicator species, with a preference for high-latitude sites. *Prediscosphaera intercisa* could be inferred as a warm-water indicator based on its inverse relationship with *M. decussata* through most of the observed interval; however, Santonian assemblages show that *P. intercisa* distribution was either not necessarily related to temperature, as it exhibits higher abundances in high-latitude assemblages comparable to *M. decussata* abundances, or there was not a strong temperature gradient restricting *P. intercisa* to low latitudes. If the former is true, *P. intercisa* distribution can then be inferred as an exploitation of niche space, which *M. decussata* could not fill in warm waters, since *M. decussata* had a cool-water affinity. Future research should focus on clarifying the paleoecological distribution of *Prediscosphaera* species.

Examination of CABFAC and Principal Component Analyses results determined that one factor, temperature, is responsible for the majority of variance observed within combined nannofossil assemblages from the Santonian through the Campanian. However, further analysis found that Campanian assemblages are more strongly related to temperature than Santonian assemblages. Temperature is determined to be the main factor responsible for 56.3% of the variance within Campanian assemblages, as PC1 correlates strongly with the temperature index by 86%. Within Santonian assemblages, PC2 is determined to reflect variance due to paleotemperature. PC2 and TI correlate strongly (89%); however, PC2 only accounts for 21.2% of the variance observed in Santonian assemblages. Therefore, Santonian nannofossil assemblages were mostly

driven by non-temperature dependent factors. This independence from the influence of temperature within the Santonian assemblages changes across the boundary into more strongly temperature-dependent assemblages in the lower Campanian.

The main factor responsible for 35.9% of the variance within the Santonian is unknown. Low abundances of *Biscutum* and *Zeugrhabdotus* spp. rule out the possibility that nutrient-enriched surface waters were dominating assemblages. Likewise, preservation of nannofossils as reflected in diversity values are also not correlated to PC1, and therefore, do not explain the variance observed. Although the factor responsible for the majority of the variation within Santonian assemblages cannot be explained here, the fact that temperature is only a secondary factor controlling Santonian nannofossil distributions is important.

The switch from non-thermally-driven assemblages in the Santonian to thermally driven assemblages during the early Campanian reflects an initiation of water-mass cooling that has been observed as being strongest in the late Campanian and Maastrichtian. This provinciality of assemblages is more clearly expressed in lower Campanian assemblages than in Santonian assemblages and is tied to intensified temperature gradients across the boundary. The stronger temperature gradient results in an equator-ward shift of cooler waters, and consequently a restriction of warm-water taxa to lower latitudes. The separation of high and low latitudes at 30^{o} indicates that intensified provincialism is reflected in broader latitudinal distributions of high-latitude assemblages as inferred by the relative abundances of *Micula decussata* and other temperature-indicative taxa. Compared to previous studies, in which the separation of

high and low assemblages is observed at 50^{o} in the Lower Cretaceous and at 40^{o} in the mid-Cretaceous, this provincialism continued to intensify beyond the early Campanian, ultimately resulting in the net speciation of high-latitude taxa by the Maastrichtian, when the Cretaceous reached its coldest temperatures.

REFERENCES

Barron, E. J., 1983. A warm equable Cretaceous: the nature of the problem. Earth-Science Reviews 19, 305–338.

Barron, E. J., Peterson, W., Thompson, S., Pollard, D., 1993. Past climate and the role of ocean heat transport: Model simulations for the Cretaceous. Paleoceanography 8, 785–798.

Barron, J., Larsen, B. et al., 1989. Proc. ODP, Init. Repts., 119: College Station, TX (Ocean Drilling Program), 229-288.

Blair, S.A., Watkins, D.K., 2009. High-resolution calcareous nannofossil biostratigraphy for the Coniacian/Santonian Stage boundary, Western Interior Basin. Cretaceous Research 30, 367-384.

Bolli, H. M., Ryan, W. B. F. et al., 1978. Initial Reports of the Deep Sea Drilling Project 40, Washington (US Government Printing Office), 183-356.

Bralower, T. J., Siesser, W. G., 1992. Cretaceous calcareous nannofossil biostratigraphy of Sites 761, 762, and 763, Exmouth and Wombat Plateaus, Northwest Australia. In: von Rad, U., Haq, B. U. et al., 1992. Proc. of ODP, Sci. Results 122, 529- 556.

Bukry, D., 1973. Coccolith stratigraphy, Leg 10, Deep Sea Drilling Project. In: Worzel, J. L. et al., 1973. Init. Repts. DSDP 10, 385-406.

Bukry, D., 1975. Coccolith and silicoflagellate stratigraphy, Northwestern Pacific Ocean, Deep Sea Drilling Project Leg 32. In: Larson, R. L. et al. 1975. Init. Repts. DSDP 32, 677-701.

Burnett, J., 1998. Upper Cretaceous. In: Bown, P.R., (Ed.), Calcareous Nannofossil Biostratigraphy. Chapman and Hall, Cambridge, 132-199.

Cepek, P., 1977. Mesozoic calcareous nannoplankton of the Eastern North Atlantic, Leg 41. In: Lancelot, Y. et al. 1977. Init. Repts. DSDP 41, 667-687.

Chang, Yi-Maw, 1967. Accuracy of fossil percentage estimation. Journal of Paleontology 41, 500–502.

Erba, E., 1992. Middle Cretaceous calcareous nannofossils from the western Pacific (ODP Leg 129): evidence for palaeoequatorial crossings. Proceedings of the Ocean Drilling Program, Scientific Results 129, 189–201.

Gartner Jr, S., 1968. Coccoliths and related calcareous nannofossils from Upper Cretaceous deposits of Texas and Arkansas. Protista 48, 1–56.

Hammer, Ø., Harper, D. A. T., Ryan, P. D., 2001. PAST: Paleontological Statistics Software Package for Education and Data Analysis. Palaeontologia Electronica 4, 9. http://palaeo-electronica.org/2001_1/past/issue1_01.htm, 5-27-2009.

Haq, B. U., Von Rad, U., O'Connell, S. et al., 1990. Proceedings of the Ocean Drilling Program, Initial Reports, 122: College Station, TX (Ocean Drilling Program), 213-288.

Hay, W. W., 2008. Evolving ideas about the Cretaceous climate and ocean circulation. Cretaceous Research 29, 725-753.

Hay, W. W., DeConto, R., Wold, C. N., Wilson, K. M., Voigt, S., Schulz, M., Wold-Rossby, A., Dullo, W. -C., Ronov, A. B., Balukhovsky, A. N., E. Soeding, 1999. Alternative global cretaceous paleogeography. In: Barrera, E., Johnson, C., (Eds.*),* The Evolution of Cretaceous Ocean/Climate Systems. Geological Society of America Special Paper 332, 1-47.

Huber, B. T., Watkins, D. K., 1992. Biogeography of Campanian-Maastrichtian calcareous plankton in the region of the Southern Ocean: Paleogeographic and paleoclimatic implications. The Antartic Paleoenvironment: A perspective on global change, Antarctic research series 56, 31-60.

Jarvis, I., Gale, A. S., Jenkyns, H. C., Pearce, M. A., 2006. Secular variation in Late Cretaceous carbon isotopes: a new $\delta^{13}C$ carbonate reference curve for the Cenomanian–Campanian (99.6–70.6 Ma). Geology Magazine 143, 561-608.

Kita, Z., A., 2015. Calcareous nannofossils from the Niobrara formation (Upper Cretaceous) Western Interior Seaway, USA. [Ph. D. Dissertation]: Lincoln, University of Nebraska-Lincoln. 96 p.

Lancelot, Y., Seibold, E. et al., 1977. Initial Reports of the Deep Sea Drilling Project 41, Washington (US Government Printing Office), 327-420.

Larson, R. L., Moberly, R. et al., 1975a. Initial Reports of the Deep Sea Drilling Project 32, Washington (US Government Printing Office), 75-158.

Larson, R. L., Moberly, R. et al., 1975b. Initial Reports of the Deep Sea Drilling Project 32, Washington (US Government Printing Office), 233-293.

Larson, R. L., Schlanger, S. O. et al., 1981. Initial Reports of the Deep Sea Drilling Project 61, Washington (US Government Printing Office), 19-394.

Lees, J., A., 2002. Calcareous nannofossil biogeography illustrates palaeoclimate change in the Late Cretaceous Indian Ocean. Cretaceous Research 23, 537-634.

Mitchell, K., L., 2012. Plankton evolution driven by paleoceanographic change: *Prediscosphaera* from the mid-Cretaceous in the Western North Atlantic. [M.S. thesis]: Lincoln, University of Nebraska-Lincoln. 75 p.

Ogg, J., Hinnov, L., Huang, C., 2012. Chapter 27 – Cretaceous. In: The Geologic Time Scale 2012. Elsevier, Boston, MA, 793–853.

Pearson, P.N., Ditchfield, P.W., Singano, J., Harcourt-Brown, K.G., Nicholas, C.J., Olsson, R.K., Shackleton, N.J., Hall, M.A., 2001. Warm tropical sea surface temperatures in the Late Cretaceous and Eocene epochs. Nature 413, 481-487.

Perch-Nielsen, K., 1977. Albian to Pleistocene calcareous nannofossils from the Western South Atlantic, DSDP Leg 39. In: Supko, P. R., et al. 1977. Init. Repts. DSDP 39, 699-823.

Perch-Nielsen, K., 1985. Mesozoic calcareous nannofossils. In: Bolli. H. M., Saunders, J. B., Perch-Nielsen, K., (Eds), Plankton Stratigraphy*:* Cambridge (Cambridge University Press), 329-426.

Pospichal, J. J., Wise, S. W., 1990. Calcareous nannofossils across the K/T boundary, ODP Hole 690C, Maud Rise, Weddell Sea. Proc. Ocean Drill. Program Sci. Results 113, 515 – 532.

Proto Decima, F., Medizza, F., Todesco, L., 1978. Southeastern Atlantic Leg 40 calcareous nannofossils. In: Bolli, H. M. et al., 1978. Init. Repts. DSDP 40, 571-634.

Roth, P. H., 1973. Calcareous nannofossils – Leg 17 Deep Sea Drilling Project. In: Winterer, E. L. et al., 1973. Init. Repts. DSDP 17, 695-795.

Roth, P.H., Bowdler, J.L., 1981. Middle Cretaceous calcareous nannoplankton biogeography and oceanography of the Atlantic Ocean. Society of Economic Paleontologists and Mineralogists, Special Publication 32, 517–546.

Roth, P.H., Krumback, K.R., 1986. Middle Cretaceous calcareous nannofossil biogeography and preservation in the Atlantic and Indian oceans: implications for palaeoceanography. Marine Micropaleontology 10, 235–266.

Schlich, R., Wise, S. W., Jr. et al., 1989. Proc. ODP, Init. Repts. 120: College Station, TX (Ocean Drilling Program), 277-337.

Sissingh, W., 1977. Biostratigraphy of Cretaceous calcareous nannoplankton. Geologie en Mijnbouw 56, 37-65.

Street, C., Bown, P., 2000. Palaeobiogeography of early Cretaceous (Berriasian–Barremian) calcareous nannoplankton. Marine Micropaleontology 39, 265–291.

Supko, P. R., Perch-Nielsen, K. et al., 1977. Initial Reports of the Deep Sea Drilling Project 39, Washington (US Government Printing Office), 231-327.

Thierstein, H.R., 1981a. Late Cretaceous nannoplankton and the change at the Cretaceous-Tertiary Boundary. In: SEPM Special Publication 32, 355-394.

Thierstein, H. R., 1981b. Calcareous nannofossil biostratigraphy, Nauru Basin, Deep Sea Drilling Project Site 462, and Upper Cretaceous nannofacies. In: Larson, R. L. et al., 1981. Init. Repts. DSDP 61, 475-494.

Watkins, D.K., 1989. Nannoplankton productivity fluctuations and rhythmically-bedded pelagic carbonates of the Greenhorn Limestone (Upper Cretaceous). Palaeogeography, Palaeoclimatology, Palaeoecology 74, 75–86.

Watkins, D. K., 1992. Upper Cretaceous nannofossils from Leg 120, Kerguelen Plateau, Southern Ocean. In: Wise, S. W., Jr., Schlich, R. et al., 1992. Proc. ODP Sci. Results 120, 343 – 370.

Watkins, D. K., Bergen, J. A., 2003. Late Albian adaptive radiation in the calcareous nannofossil genus Eiffellithus. Micropaleontology 49, 231-251.

Watkins, D.K., Self-Trail, J.M., 2005. Calcareous nannofossil evidence for the existence of the Gulf Stream during the late Maastrichtian. Paleoceanography 20, 1-9.

Watkins, D. K., Wise, S. W. Jr., Popsichal, J. J., Crux, J., 1996. Upper Cretaceous calcareous nannofossil biostratigraphy and paleoceanography of the Southern Ocean. Papers in the Earth and Atmospheric Sciences 258. 355-381.

Wei, W., Thierstein, H. R., 1989. Upper Cretaceous and Cenozoic calcareous nannofossils of the Kerguelen Plateau (Southern Indian Ocean) and Pryds Bay (East Antarctica). In: Barron, J., Larsen, B. et al., 1991. Proc. ODP Sci. Results 119, 467-493.

Williams, J.R., Bralower, T.J., 1995. Nannofossil assemblages, fine fraction stable isotopes, and the palaeoceanography of the Valanginian–Barremian (Early Cretaceous) North Sea Basin. Palaeoceanography 10, 815–839.

Wind, F. H., 1979. Maastrichtian-Campanian nannoflora provinces of the southern Atlantic and Indian oceans. In: Talwani, M., Hay, W. W., Ryan, B. F., (Eds.), Deep Sea Drilling Results in the Atlantic Ocean: Continental Margins and Paleoenvironment, Maurice Ewing Ser., 3, 123 – 137, AGU, Washington, D. C.

Winterer, E. L., Ewing, J. I. et al., 1973. Initial Reports of the Deep Sea Drilling Project 17, Washington (US Government Printing Office), 145-234.

Wise, S., 1983. Mesozoic and Cenozoic calcareous nannofossils recovered by Deep-Sea Drilling Project Leg-71 in the Falkland Plateau region, Southwest Atlantic-ocean. Initial Reports of the Deep Sea Drilling Project 71, Washington (US Government Printing Office), 481–550.

Worzel, J. L., Bryant, W. et al., 1973. Initial Reports of the Deep Sea Drilling Project 10, Washington (US Government Printing Office), 259-295.

FIGURES

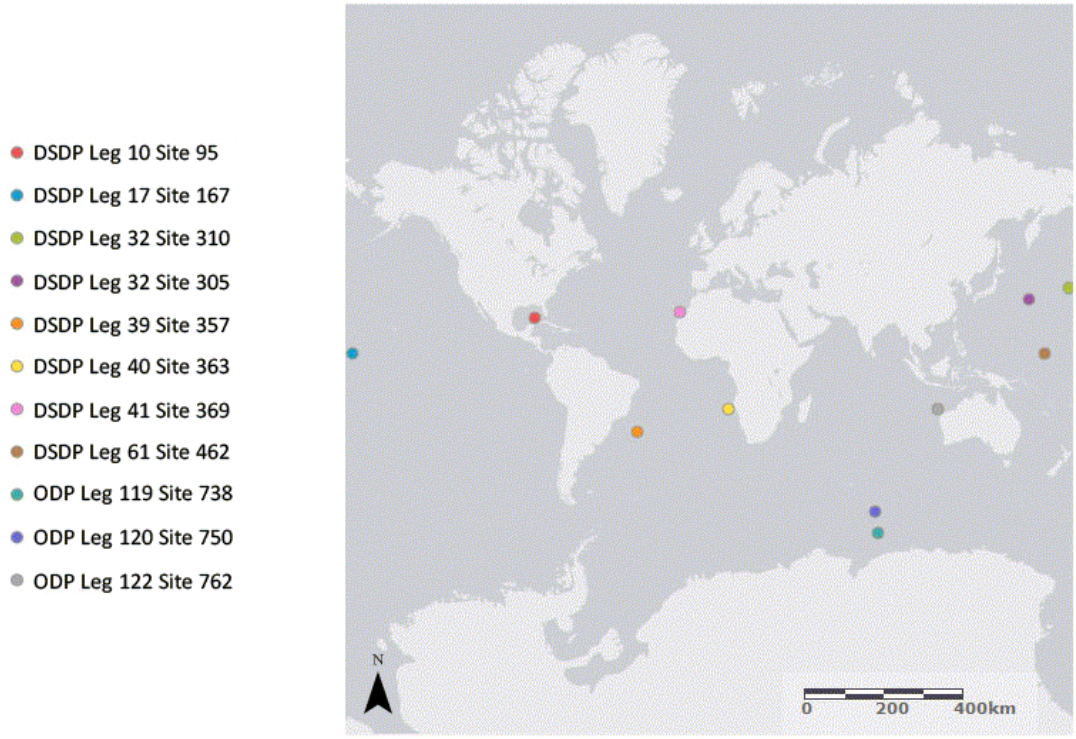

Figure 1. Locality map illustrating current positions of all studied DSDP/ODP sites.

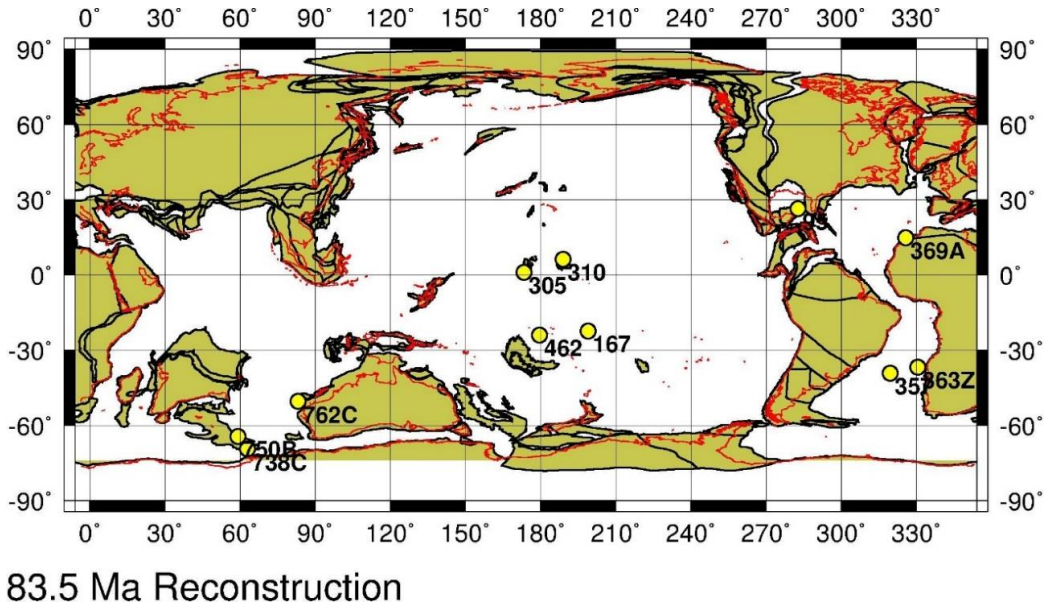

Figure 2. Paleogeographic reconstruction showing positions for all localities at the Santonian-Campanian boundary.

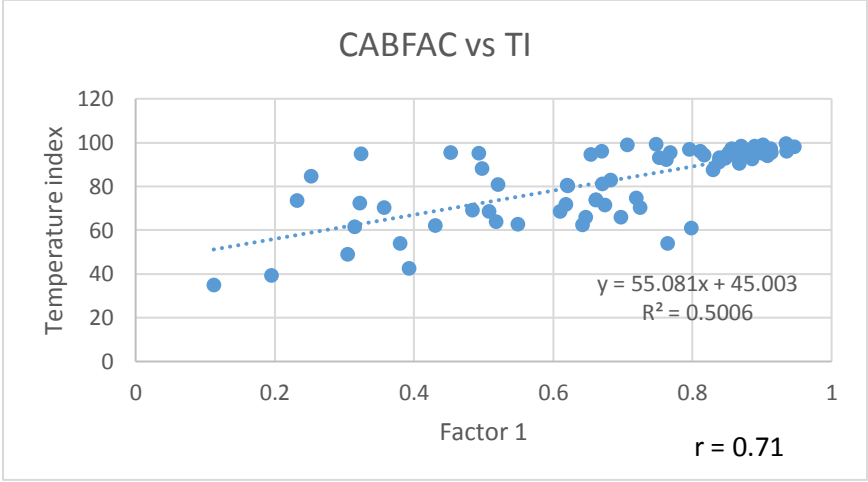

Figure 3. Correlation plot of Factor 1 from the CABFAC factor analysis against TI values of all data. The strong correlation implies that paleotemperautre is the factor responsible for the majority of the variation within assemblages.

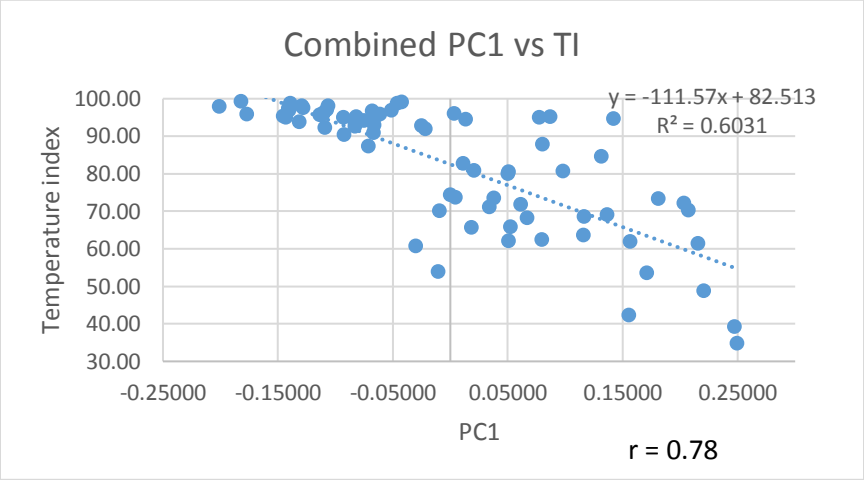

Figure 4. Correlation plot of Principal Component 1 against TI values of all data. Similar to the CABFAC results for all data, the strong correlation implies that paleotemperature is the main factor responsible for variance observed.

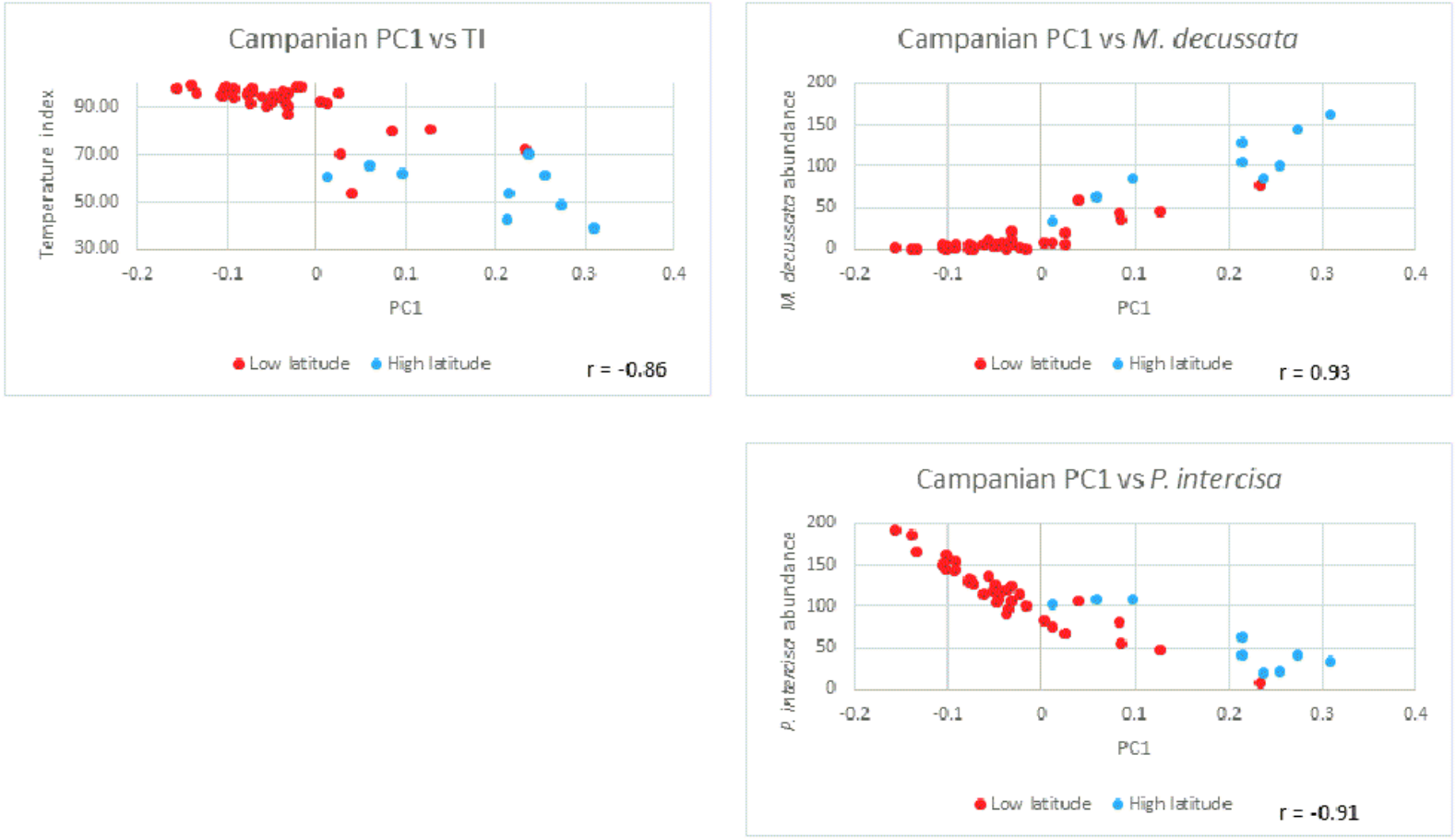

Figure 5. Campanian correlation plots. The high correlation of Principal Component 1 values to TI suggests that the main factor controlling variation is related to paleotemperature. The strong correlation to *M. decussata* (cool-water indicator), and the strong inverse correlation to *P. intercisa* implies that changes in temperature are reflected by the relative abundances of these two species.

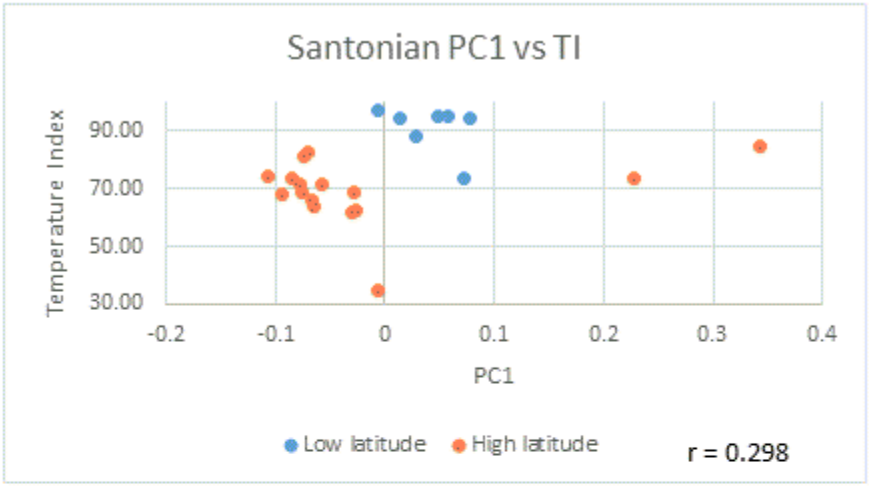

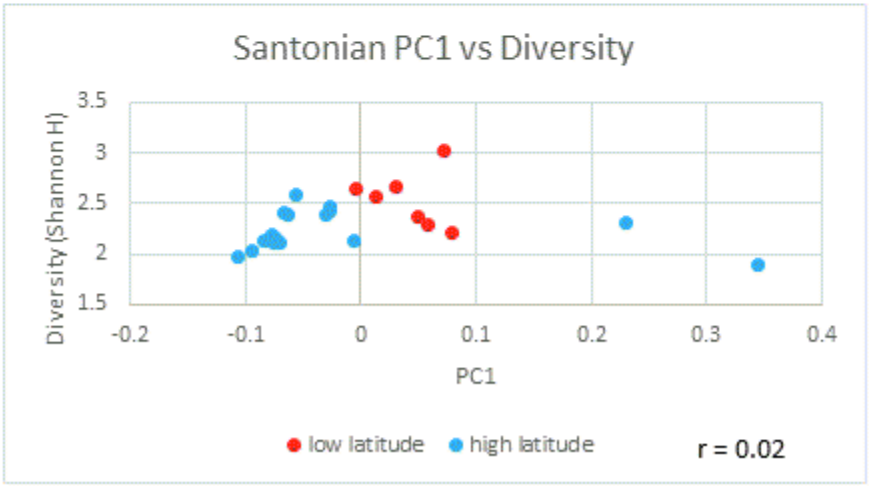

Figure 6. Santonian Principal Component 1 correlation plots. PC1 values are not highly correlated to the TI. The low correlation implies that the variance observed is probably not related to paleotemperature. Likewise, Diversity values are not correlated to PC1 values. When the two high-latitude outliers are removed, the correlation coefficient only increases to 0.57; therefore, diversity is not inferred as the factor controlling variance in the Santonian.

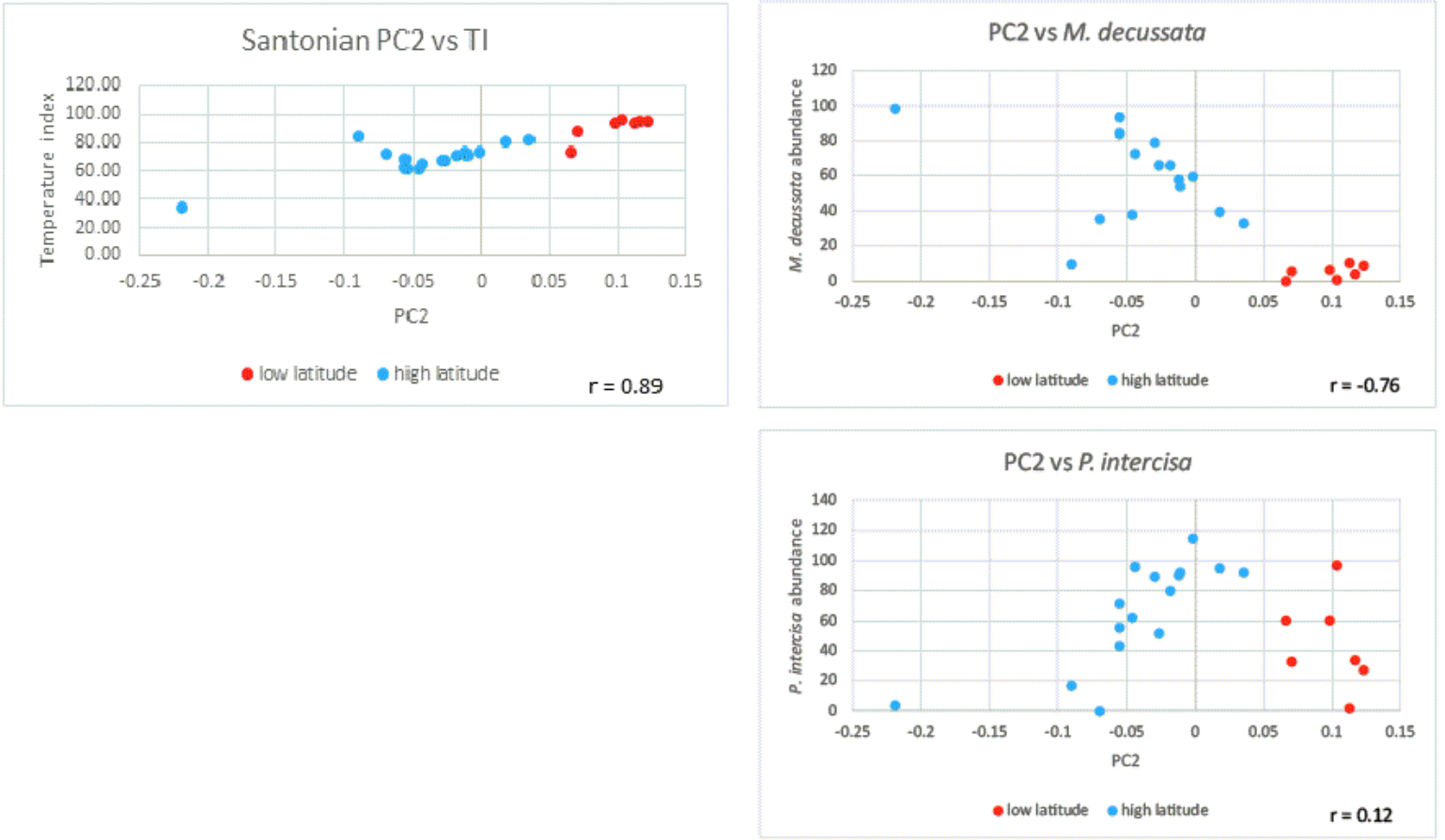

Figure 7. Santonian Principal Component 2 correlation plots. PC2 values are strongly correlated to TI values and to the cool-water indicator *M. decussata*; therefore, PC2 is inferred to be reflecting changes related to paleotemperature. *P. intercisa* does not show a linear trend when compared to PC2, suggesting its distribution is not controlled by temperature in the Santonian, as it appears to have been in the Campanian.

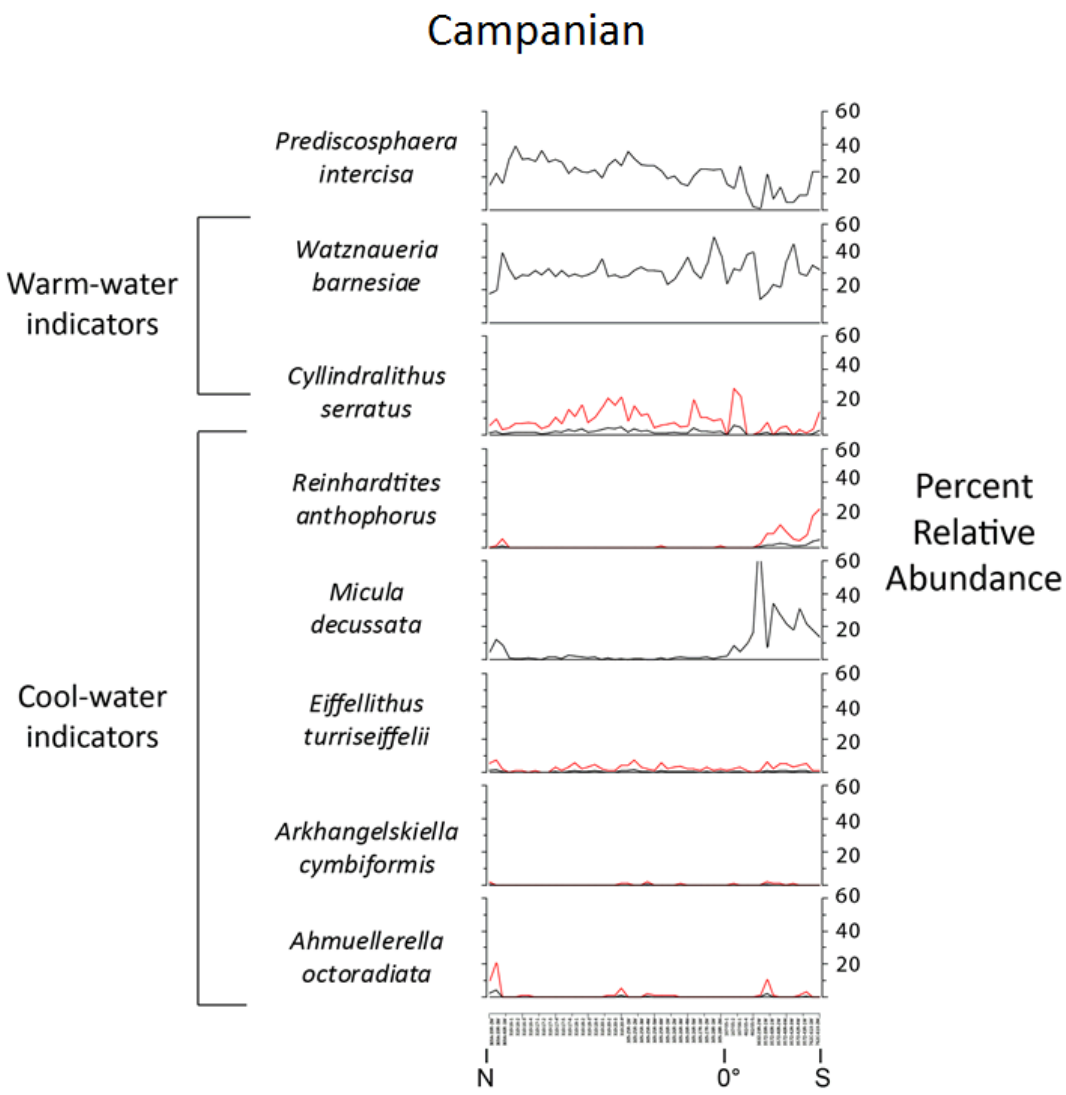

Figure 8. % abundance of temperature indicative species by latitude in the Campanian. Red lines are 5X exaggeration. *W. barnesiae, E. turriseiffelii,* and *A. cymbiformis* do not demonstrate a latitudinal trend. *C. serratus* exhibits higher abundances in lower latitudes, indicative of warm surface waters. *R. anthophorus* and *M. decussata* exhibit higher abundances in high latitudes, indicative of cool surface waters. *P. intercisa* was not used in the temperature index, but shows relatively higher abundances in lower latitudes.

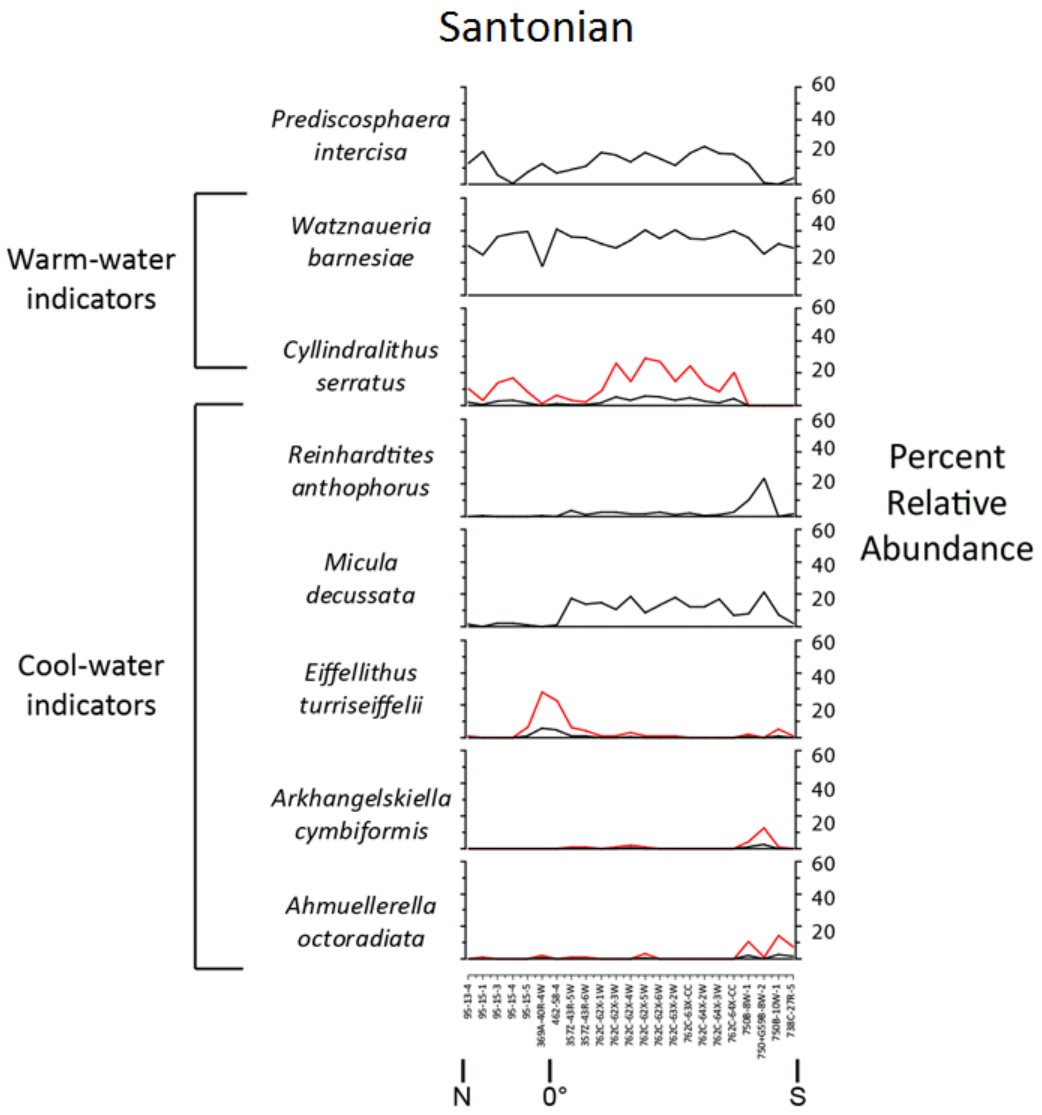

Figure 9. % abundance of temperature indicative species by latitude in the Santonian. Red lines are 5X exaggeration. *W. barnesiae* does not exhibit a latitudinal trend. *E. turriseiffelii* is most abundant in the lowest latitudes, opposite of its expected trend. The rest of the cool-water indicators exhibit higher abundances in high latitudes. *C. serratus* and *M. decussata* exhibit higher abundances across broad latitudes, indicating a weak latitudinal temperature gradient, relative to their strong temperature-driven Campanian distributions.

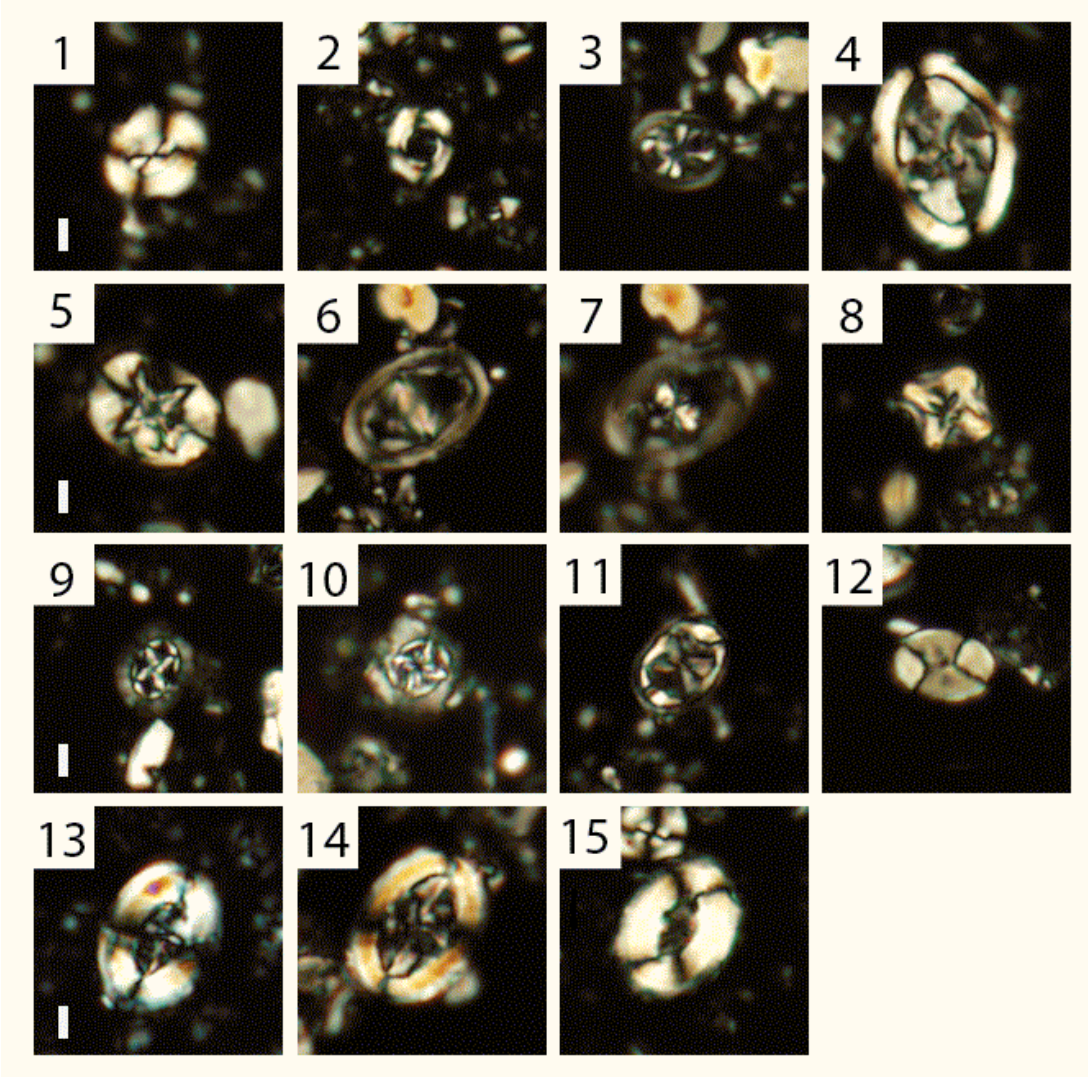

Figure 10. Upper Cretaceous species discussed in this study. Images 1-8 are species used in the calculation of the TI. Images 11-15 are species discussed in age assignments. Image 9 compares *Prediscosphaera intercisa* to Image 10, *Prediscosphaera cretacea*. Images 1, 2, 4-8, and 11 are from Sample 357-39R-1W, 36-37cm. Image 3 is from sample 750B-10W-1, 48-50cm. Image 9 is from Sample 369A-40R-1W, 130-131cm. Image 10 is from Sample 738C-27R-5, 67-68cm. Images 12 and 13 are from Sample 369A-39R-3W, 111-112cm. Image 14 is from Sample 762C-62X-1, 45-46cm. All images were photographed using crossed polarizers. Scale bars are 2 µm.

1. Watznaueria barnesiae; 2. Cylindralithus serratus; 3. Ahmuellerella octoradiata; *4. Arkhangelskiella cymbiformis*; *5. Eiffellithus turriseiffelii*; *6-7. Reinhardtites anthophorus*; *8. Micula decussata*; *9. Prediscosphaera intercisa*; *10. Prediscosphaera cretacea*; *11. Helicolithus trabeculatus; 12. Calculites obscurus*; *13. Aspidolithus parcus parcus*; *14. Aspidolithus parcus expansus; 15*. Aspidolithus parcus *constrictus*

Table 1. Summary of sites chosen for this study. Samples were created from sediment intervals of interest, which were selected based on information within preliminary reports. Citations are included in the table.

ODP/DSDP	Location	Latitude and Longitude	Interval of interest	Lithology
Leg 10 Site 95	Gulf of Mexico, Yucatan Shelf	24.15, -86.3975	Cores 13-15	Burrowed nannofossil chalk and ooze and foram-nanno chalk (Worzel et al., 1973).
Leg 39 Site 357	Rio Grande Rise, South Atlantic Ocean	-30.0042, -35.5598	Cores 39-43	Micritic chalk, marly limestone, marly foram-nanno limestone (Supko et al., 1977).
Leg 40 Site 363	Angola Basin, South Atlantic Ocean	-19.6458, 9.046667	Cores 23-25	Marly nannofossil chalk (Bolli et al., 1978).
Leg 41 Site 369 Hole A	Cape Bojador, North Atlantic Ocean	26.59167, -14.9833	Cores 39-40	Argillaceous chalk with minor chert (Lancelot et al., 1977).
Leg 17 Site 167	Magellan Rise, Pacific Ocean	7.068333, -176.825	Cores 55-59	Nannofossil chalk (ground up in Core 55), marly limestone (Winterer et al., 1973).
Leg 32 Site 305	Shatsky Rise, Pacific Ocean	32.00217, 157.85	Cores 25-27	Nanno ooze and chalk, foram-nanno chalk and ooze (Larson et al., 1975a).
Leg 32 Site 310	Hess Rise, Pacific Ocean	36.8685, 176.901	Lithologic Subunit 4a, Cores 16-21	Nannofossil ooze and chert (Larson et al., 1975b).
Leg 61 Site 462	Nauru Basin, Pacific Ocean	7.2375, 165.0305	Lithologic Unit III, Cores 55-58	Claystone and marlstone, zeolitic claystone, redeposited volcaniclastic sandstone, zeolitic claystone/mudstone with one section (58-4) of nanno-marlstone (Larson et al., 1981).
Leg 120 Site 750 Hole B	Kerguelen Plateau, Southern Ocean	-57.592, 81.2395	Lithologic Subunit IIIB, Cores 8W-10W	Intermittently silicified limestone, chalk, and chert (Schlich et al., 1989).
Leg 122 Site 762 Hole C	Exmouth Plateau, Indian Ocean	-19.8872, 112.254	Lithologic Subunit IVC, Cores 61-64.	Foraminifera-bearing nannofossil chalk interbedded with nannofossil claystone (Haq et al., 1990).
Leg 119 Site 738 Hole C	Southern Kerguelen-Heard Plateau, Southern Ocean	-62.709, 82.7875	Lithologic Units V-VI, Cores 24-29	Calcareous chalk with chert, limestone with minor clay and chert (Barron et al., 1989).

Table 2. Summarization of each site's sections from which samples were produced. Poor preservation resulted in barren or essentially barren samples with too few nannofossils to count.

Locality	Water depth	Sections used to produce samples	Sections with counted samples	Uncounted samples
10-95	1633 m	13-1,2,3,4; 14-1; 15-1,2,3,4,5,6	13-4; 15-1,3,4,5	13-1,2,3; 14-1; 15-2,6
17-167	3166 m	55-1,2; 56-1; 57-1; 58-2,3,4; 59-1,3	55-1,2; 56-1	57-1; 58-2,3,4; 59-1,3
32-305	2903 m	25-1,2,3,4,5,6; 26-1,2,3,4,5; 27-1,2; 28-1,2	25-1,2,3,4,5,6; 26-1,2,3,4,5; 27-1,2; 28-1,2	
32-310	3516 m	16-1,2,3,4; 17-1,2,3,4,5,6; 18-1,2,3,4; 20-1,2,3,4; 21-1,2	16-1,2,3,4; 17-1,2,3,4,5,6; 18-1,2,3,4; 20-1,2,3,4	21-1,2
39-357	2086 m	39-1; 40-1,2,3,4,5,6; 41-1x2,2,3,4,5; 42-1,2,3,4,5; 43-1,2,3,4,5,6	39-1; 40-1,2,6; 42-3,4; 43-1,5,6	40-3,4,5; 41-1x2,2,3,4; 42-1,2,5; 43-2,3,4
40-363	2248 m	23-1,2; 24-1,2; 25-1,2	23-2	23-1; 24-1,2; 25-1,2
41-369A	1752 m	39-1,2,3; 40-1,2,4	39-2,3; 40-1,4	39-1; 40-2
61-462	5189 m	55-1,2,3,4,5; 56-1,2; 57-1,2,3,CC; 58-1,2,3,4,5,CC	55-4,5; 58-4	55-1,2,3; 56-1,2; 57-1,2,3,CC; 58-1,2,3,5,CC
119-738C	2253 m	24R-1,2,3; 25R-1,2,3,4; 26R-1,2,3; 27R-1,2,3,4,5; 28R-1,2,3,4; 29R-1,2,3	27R-5	24R-1,2,3; 25R-1,2,3,4; 26R-1,2,3; 27R-1,2,3,4; 28R-1,2,3,4; 29R-1,2,3
120-750B	2031 m	8W-1,2; 9W-1,2; 10W-1	8W-1,2; 10W-1	9W-1,2
122-762C	1360 m	61x-1,2; 62x-1,2,3,4,5,6; 63x-1,2,3,CC; 64x-1,2,3,4,CC	61x-1,2; 62x-1,3,4,5,6; 63x-2,CC; 64x-2,3,CC	62x-2; 63x-1,3; 64x-1,4
		Total samples produced: 151	Total samples counted: 74	Total samples not counted: 77

Table 3. Age assignments of sections based on species present in samples. Ages were assigned based on the presence of: *Aspidolithus parcus parcus* for lower Campanian; *Ceratolithoides* and *Uniplanarius* spp. for mid-upper Campanian, and the absense of these species for Santonian.

Santonian	Lower Campanian	Mid-upper Campanian
95-13-4; -15-1,-3,-4,-5	310-20-2,3,4	310-16-1,-2,-3,-4; -17-1,-2,-3,-4,-5,-6; -18-1,-2,-3,-4; -20-1
369A-40R-4W	305-28R-1W,2W	
462-58-4	369A-40R-1W	305-25R-1W,-2W,-3W,-4W,-5W, -6W; -26R-1W,-2W,-3W,-4W, -5W; -27R-1W,-2W
357Z-43R-5W,6W	462-55-4,5	
762C-62X-1W,3W,4W,5W,6W; -63X-2W,CC; -64X-2W,3W,CC	357Z-39R-1W; -40R-1W,2W,6W; -42R-3W,4W; -43R-1W	369A-39R-2W,-3W
750B-8W-1,2; -10W-1	762C-61X-1W,2W	167-55-1,-2; -56-1
738C-27R-5		363Z-23R-2W

Authorities of species considered in this study are listed in alphabetical order:

Ahmuellerella octoradiata (Górka 1957) Reinhardt & Górka 1967

Arkhangelskiella cymbiformis Vekshina, 1959

Aspidolithus parcus subsp*. constrictus* (Hattner et al., 1980) Perch-Nielsen, 1984

Aspidolithus parcus expansus (Wise & Watkins in Wise, 1983) Perch-Nielsen, 1984

Aspidolithus parcus parcus (Stradner, 1963) Noël, 1969

Calculites obscurus (Deflandre, 1959) Prins and Sissingh *in* Sissingh, 1977

Ceratolithoides aculeus (Stradner, 1961) Prins & Sissingh *in* Sissingh, 1977

Cribrosphaerella ehrenbergii (Arkhangelsky, 1912) Deflandre *in* Piveteau, 1952

Cylindralithus serratus (Bramlette and Martini, 1964) Stover, 1966

Eiffellithus turriseiffelii (Deflandre *in* Deflandre and Fert, 1954) Reinhardt, 1965

Eprolithus floralis (Stradner, 1962) Stover, 1966

Helicolithus trabeculatus (Górka, 1957) Verbeek, 1977

Marthasterites furcatus (Deflandre in Deflandre & Fert, 1954) Deflandre, 1959

Micula decussata (Gardet, 1955) Vekshina, 1959

Prediscosphaera cretacea (Arkhangelsky, 1912) Gartner, 1968

Prediscosphaera intercisa (Deflandre *in* Deflandre and Fert, 1954) Shumenko, 1976

Reinhardtites anthophorus (Deflandre, 1959) Perch-Nielsen, 1968

Uniplanarius gothicus (Deflandre, 1959) Hattner & Wise, 1980

Watznaueria barnesiae (Black *in* Black and Barnes, 1959) Perch-Nielsen, 1968

Genera discussed:

Biscutum Black *in* Black & Barnes, 1959

Ceratolithoides Bramlette & Martini, 1964

Prediscosphaera Vekshina, 1959

Uniplanarius Hattner & Wise, 1980

Zeugrhabdotus Reinhardt, 1965